


ORIGINAL ARTICLE

Combination of resveratrol-containing collagen with adipose stem cells for craniofacial tissue-engineering applications

Chih-Chien Wang¹ | Chih-Hsin Wang² | Hsiang-Cheng Chen³ | Juin-Hong Cherng^{4,5,6} |
Shu-Jen Chang³  | Yi-Wen Wang⁴ | Adrienne Chang⁷ | Jue-Zong Yeh⁸ | Yi-Huei Huang⁹ |
Cheng-Che Liu¹⁰

¹Department of Orthopedic Surgery, Tri-Service General Hospital, National Defense Medical Center, Taipei, Taiwan (R.O.C.)

²Department of Plastic and Reconstructive Surgery, Tri-Service General Hospital, National Defense Medical Center, Taipei, Taiwan (R.O.C.)

³Division of Rheumatology/Immunology/Allergy, Department of Internal Medicine, Tri-Service General Hospital, National Defense Medical Center, Taipei, Taiwan (R.O.C.)

⁴Department and Graduate Institute of Biology and Anatomy, National Defense Medical Center, Taipei, Taiwan (R.O.C.)

⁵General Clinical Research Center for New Drug Trial, Tri-Service General Hospital, National Defense Medical Center, Taipei, Taiwan (R.O.C.)

⁶Department of Gerontological Health Care, National Taipei University of Nursing and Health Sciences, Taipei, Taiwan (R.O.C.)

⁷Department of Chemistry, New York University, Abu Dhabi, United Arab Emirates

⁸Department of Pharmacy Practice, Tri-Service General Hospital, National Defense Medical Center, Taipei, Taiwan (R.O.C.)

⁹Biomedical Engineering Program, Graduate Institute of Applied Science and Technology, National Taiwan University of Science and Technology, Taipei, Taiwan (R.O.C.)

¹⁰Department of Physiology and Biophysics, Graduate Institute of Physiology, National Defense Medical Center, Taipei, Taiwan (R.O.C.)

Correspondence

Cheng-Che Liu, PhD, Department of Physiology and Biophysics, Graduate Institute of Physiology, National Defense Medical Center, R6104, No. 161, Section 6, Minquan East Road, Neihu District, Taipei 11490, Taiwan. (R.O.C.)
Email: chencheliu2002@gmail.com

Repair and regeneration of craniofacial tissues is particularly challenging because they comprise a complex structure of hard and soft tissues involved in intricate functions. This study combined collagen scaffolds and human adipose stem cells (hASCs) for oral mucosal and calvarial bone regeneration by using resveratrol (RSV), which affects the differentiation of mesenchymal stem cells. We have evaluated the effect of collagen scaffold-containing RSV (collagen/RSV) scaffolds both in vitro and in vivo for their wound healing and bone regeneration potential. Scanning electron microscopy and immunostaining results reveal that hASCs adhere well to and proliferate on both collagen scaffolds and collagen/RSV scaffolds. Oral mucosal lesion experiments demonstrated that the collagen/RSV scaffold is more effective in wound closure and contraction than the collagen scaffold. The micro-computed tomography (μ CT) images of calvarial bone display regenerating bone in defects covered with hASCs on collagen/RSV scaffolds that are more visible than that in defects covered with hASCs on a collagen scaffolds. RSV was more effective at inducing hASC differentiation on the collagen scaffold, suggesting that collagen/RSV scaffolds can provide useful biological cues that stimulate craniofacial tissue formation.

KEYWORDS

biocompatibility, bone regeneration, collagen, oral mucosal, resveratrol

Funding information

Defense Technology Cooperative Research, Grant/Award number: 105-2623-E-016-004-D; Tri-Service General Hospital ROC program, Grant/Award numbers: TSGH-C103-037, TSGH-C97-109, TSGH-C99-129, TSGH-C104-098, TSGH-C106-074; Ministry National Defense-Medical Affairs Bureau, Grant/Award number: MAB-105-041

1 | INTRODUCTION

Defects in craniofacial tissues resulting from trauma, congenital abnormalities, oncological resection, or progressive deforming diseases present formidable challenges to surgeons.^{2,3} Restoration of these tissues is therefore a subject of clinical, scientific, and engineering investigations.⁴ Craniofacial tissues often need repair because of structural deficiencies, but replacing the craniofacial structure is difficult because of its complex functions, which is based on an intricate three-dimensional (3D) structure consisting of soft and hard tissues.² Surgical treatment of periodontal and other craniofacial defects is, therefore, unpredictable and, in many cases, does not restore full function to the tissues. Consequently, structure, function, aesthetics, and pain associated with the process of bone repair and regeneration must be taken into consideration. This need gives rise to treatment challenges that are often more complex than those for other parts of the body.

Hard tissues such as the craniofacial skeleton and teeth are formed by the extracellular matrix (ECM). The ECM is composed of collagen and elastic fibres and is regenerated by specific osteoblast and osteoclast interactions.⁵ Presently, massive bone defects can be treated with synthetic or natural biomaterials that promote the migration, proliferation, and differentiation of bone cells. However, these cells lack the osteogenetic and osteoinductive properties of bone autografts; consequently, researchers have begun turning to tissue engineering in search of alternative solutions.⁶

The basic premise of tissue engineering is that controlled manipulation of the extracellular microenvironment can enable control over the cells' ability to organize, grow, and differentiate into a functional ECM and become new working tissue. This is a complex process that requires autocrine, paracrine, and endocrine signals; positional cues, cell-matrix interactions; mechanical forces; and cell-cell contacts that mediate the formation of 3D tissue. To engineer functional tissues, host and donor cells must be provided with appropriate spatial and temporal cues, which enable the growth, differentiation, and synthesis of an ECM with sufficient volume and functional integrity. There have been many advances in oral and craniofacial tissue engineering in the last decade arising from combinations of biomaterials, stem cells, and recombinant growth factors, including

Key Messages

- using collagen/RSV biocomposite scaffolds in stem cell differentiation, we demonstrate for the first time that RSV is highly biocompatible and yields high differentiation rates of stem cells and osteogenesis in epithelium-inducing media *in vitro*
- eight-week-old male Sprague-Dawley rats¹ were used to test the effects of collagen/RSV scaffold on hASCs-based bone regeneration for repairing calvarial defects
- RSV-containing collagen biomaterials are more effective than the collagen scaffolds at enhancing the epithelial and osteogenic differentiation of hASCs; this study developed a feasible procedure for future clinical applications using collagen/RSV scaffolds for tissue engineering for craniofacial defect reconstruction

in vitro and *in vivo* engineering of craniofacial bone,^{7,8} cranial sutures,¹ periodontium,⁹ oral mucosa,¹⁰ tooth-associated structures,¹¹ and the temporomandibular joint.¹² Clinical studies have successfully used collagen scaffolds to treat oral cavity disease and have shown good haemostasis, adherence, and significant epithelialisation at 1 and 3 months for lesion sites covered with collagen scaffolds.

Adipose-derived stem cells (ASCs), which are typically obtained via lipoaspirate, can be expanded in culture and differentiated into a variety of cell types. There are numerous strategies for adipose tissue engineering and culture in which core tissue engineering principles are optimised using appropriate cells, scaffolds, and microenvironments.^{13,14} The scientists have shown that human adipose stem cells (hASCs) seeded on a silk fibroin-chitosan scaffold enhance wound healing and are capable of differentiating into fibrovascular, endothelial, and epithelial components of restored tissue.¹⁵ ASCs are widely used in craniofacial reconstruction, particularly in engineering adipose and bone tissues. Moreover, ASCs and osteoinductive proteins have been hypothesised to augment bone regeneration.^{16,17} In a German study, human-derived ASCs were combined with bone chips from the iliac crest and then used to regenerate a large calvarial defect to near complete continuity in a 7-year-old patient.¹⁸ Because human ASCs are multi-potent, available in large quantities per individual, and transplantable in an

autologous setting, they can be an ideal cell source for oral-tissue engineering.

When the mucosa is injured, cell apoptosis and DNA damage occur. Simultaneously, the damage induces inflammatory signal pathways such as those involving tumour necrosis factor alpha and interleukin 6, which activate inflammatory cells that clean the affected area. Wound repair is a complex process involving the orchestrated interaction of multiple growth factors, cytokines, chemokines, and cell types. Inflammatory cells inside the wound area produce hydrogen peroxide (H_2O_2), generating reactive oxygen species (ROS) that induce the expression of growth factors such as transformation growth factor beta and platelet-derived growth factor, which synthesise collagen and blood vessels for wound healing.¹⁹ An excess of ROS or a lack of cell antioxidants (catalases, dismutase, peroxidases, and glutathione) contributes to oxidative stress, which, in turn, damages mitochondrial DNA, proteins, and scaffolds and leads to cell death and tissue damage. Furthermore, the ROS generated by both neutrophils and macrophages play a central role in conferring resistance to wound infection.^{20,21} Blood coagulation, activated complement pathways, and activated parenchymal cells at the wound site generate numerous amounts of vasoactive mediators.²²

Resveratrol (RSV) is found in various plants, including grapes, berries, and peanuts. It is also present in wines, especially in red wines.²³ RSV, an antioxidant and pro-oxidant, was first discovered in food in 1940. Through animal experiments, its anticancer and anti-inflammatory functions, as well as its benefits in decreasing blood sugar and its positive effects on the cardiovascular system, have gradually been discovered. RSV can maintain the concentration of intracellular antioxidants. RSV-based treatment is also associated with a well-defined hyper-proliferative epithelial region, high cell density, enhanced deposition of connective tissue, and improved histological architecture. In addition, a reciprocal relationship exists between osteogenesis and adipogenesis, that is, the RSV and isonicotinamide have recently been shown to enhance osteogenesis, while the nicotinamide has been found to enhance adipogenesis through the activation of SIRT1. Moreover, the bone-protective effects of RSV agonist on the SIRT1 gene have highlighted this compound as a candidate for osteoporosis therapy.²³ Considered together, these studies describe an RSV mechanism that promotes the osteogenesis of hASCs by upregulating RUNX2 gene expression via the SIRT1/FOXO3A axis.²⁴ The pharmacological enrichment of hASCs for osteoprogenitors could thus potentially provide a novel treatment for critical bone defects and for regenerative medicine.^{25–27} The present study investigated the effects of RSV in combination with a collagen scaffold on hASC differentiation through *in vitro* and *in vivo* experiments on engineering tissue for the craniofacial structure.

2 | MATERIALS AND METHODS

2.1 | Materials

Type I acid-soluble collagen from calfskin (Cat. No. C3511), resveratrol (MW 228.2; Cat. No. R5010), and Masson's trichrome staining reagent (Cat. No. HT-1079 + HT-15) were obtained from Sigma Chemicals Co. (St. Louis, MO). Poly (ϵ -caprolactone) (PCL, MW 50 000; CAPA 6500) was obtained from Solvay Interco, Warrington, UK. The induction medium was first added and then topped with 5×10^4 cells evenly spread in 6 plates containing osteogenic differentiation cultivation liquid (Dulbecco's modified Eagle's medium, DMEM), 10% foetal bovine serum (FBS), 0.1 μ M dexamethasone, 50 μ M ascorbate-2-phosphate, 10 mM β -glycerophosphate, and 1% antibiotic/anti-mycotic.

2.2 | Preparation of collagen/RSV and collagen scaffolds

Collagen solution (0.25% wt/vol) was prepared by dissolving type I collagen in 1% acetic acid; aliquots (8 μ g/mL) of RSV were prepared by dissolution in 100% EtOH. The 2 solutions were mixed together to form a collagen/RSV matrix. Dissolution was facilitated by stirring with a magnetic stirrer at room temperature. Aliquots (0.275 mL) of the collagen/RSV solution were placed in a 7-mL glass vial and frozen at -20°C for approximately 60 minutes. The frozen samples were placed in a freeze dryer (Kingming, ROC) at -45°C under a 300 mbar vacuum for 24 hours. Aliquots (0.5 mL) of 2.5% wt/vol PCL/dichloromethane solution were then added to the collagen mats to prepare 1:20 wt/vol collagen/RSV biocomposites. The vials were kept closed for 30 minutes before the lids were removed to allow overnight solvent evaporation. The procedure for the preparation of collagen scaffolds is similar to that of collagen/RSV scaffolds (ie, without RSV condition).

2.3 | Control release analysis

The amount of RSV released from the fabrics was obtained after 150 minutes of immersion in RSV (pH = 7) solutions and was measured under conditions similar to human body fluids. Collagen/RSV scaffolds that had absorbed RSV were immersed in 50 mL of artificial saliva solution (Biotene, Laclede Inc., CA, USA). The solutions containing the fabrics were shaken and maintained at human body temperature ($\pm 37^\circ\text{C}$) and sampled at 0, 2, 4, 5, 10, 15, 20, 30, 60, 90, 120, and 150 minutes. RSV concentration was measured by spectrophotometry at its maximum absorbance wavelength (350 nm) using a calibration curve. The entire procedure was executed at body temperature to simulate *in vivo* conditions, and the solutions were shaken to maximise the fabric's absorption of the extract. All assays were made in triplicate.

2.4 | Coculture stem cells

2.4.1 | Isolation and purification of human adult oral adipose stem cells

Adipose tissue was collected by clinical routing surgery as certified by the Institutional Review Board of Tri-Service General Hospital, Taipei, Taiwan. Approximately 1 to 3 mL samples were isolated from adipose tissue and incubated with transfer buffer (0.1 M phosphate buffered saline, 1% penicillin/streptomycin, 0.1% glucose) and transferred immediately to our lab. The tissue was then cut into 1-mm diameter sections and transferred into 10 mL DMEM containing 0.1% collagenase for 1 day in a 37°C incubator. Tissue sections were then transferred to a DMEM/10% FBS (GIBCO, Thermo Fisher Scientific, Massachusetts) solution for 24 hours. Cells were collected by centrifugation at 500g for 5 minutes. The resulting pellet was suspended in a keratinocyte serum-free medium (K-SFM, Gibco) containing 5% FBS and antioxidants N-acetyl-cysteine and L-ascorbic acid-2-phosphate. Fifteen cells were then placed in a 25 cm² flask and incubated under 5% CO₂ at 37°C. After 2 to 4 days of incubation, depending on the cell's growth rate, the primary cells were collected after changing the medium. Under this growth condition, each generation took up to 2 to 3 days to reach confluency.^{28,29}

2.4.2 | Epithelial differentiation

The distinct pieces of collagen/RSV scaffold with a diameter of 13 mm² were stored in 24-well plates under sterile conditions, and they were sterilised by ultraviolet (UV) irradiation for 18 hours before use. Human adult stem cells (density = 4 × 10⁵ cells/cm²) were cultured using epithelial medium. We have added the keratinocyte induction medium on to the 6 plates with 5 × 10⁴ cells per well. The cultivation liquid was replaced every 7 days. After culturing the biocomposites for 14 days (n ≥ 3 individual experiments), samples were prepared for histological, immunohistochemical, and scanning electron microscopic analyses. Cell cultures were also monitored by using specific stains and antibodies against stem cells (Oct-4 and Nestin) and keratinocytes (CK-14 and Involucrin).

2.4.3 | Osteogenic differentiation

The procedure for the preparation of bone biocomposites is similar to that of epithelial cell biocomposites. That is, after collagen/RSV scaffolds were sterilised by UV irradiation for 18 hours, the human adult stem cells (density of 4 × 10⁵ cells/cm²) were cultured in stem cell to osteocyte-inducing medium. The bone biocomposites were cultured using osteogenic differentiation. We have used 6 plates containing evenly added 5 × 10⁴ cells per well and osteogenic differentiation cultivation liquid. The cultivation liquid was replaced every 2 days. After 2 weeks, we observed the plates with Alizarin red and von Kossa stain. We have used the following to prepare the osteoinduction formula:

DMEM, 10% FBS, 0.1 μM dexamethasone, 50 μM ascorbate-2-phosphate, 10 mM β-glycerophosphate, 1% antibiotic/anti-mycotic. We have used a keratinocyte induction medium of 6-well plates containing evenly added 5 × 10⁴ cells per well. The cultivation liquid is refreshed every 7 days. The medium was prepared using the keratinocyte induction formula: K-SFM, calcium chloride, bovine pituitary extract, epidermal growth factor, 1% antibiotic/anti-mycotic.

2.5 | In vivo studies

2.5.1 | Animal model of tough defect surgery

An oral mucosal defect (approximately 5 mm × 3 mm) was surgically treated in the Sprague-Dawley rats using a scalpel on the underside surface of the tongue after intra-muscular anaesthesia. Then, the epithelial cell biocomposites were attached with biocompatible mucilage. After the surgical procedure, the rats were sacrificed at 3 days (N = 3), 1 (N = 3) and 2 (N = 3) weeks after surgery.

2.5.2 | Rat in vivo crucial-sized calvarial defect procedure

Eight-week-old male Sprague-Dawley rats were used to test the effects of collagen/RSV scaffold on hASCs-based bone regeneration for repairing calvarial defects. Cells and scaffold constructs were implanted under anaesthesia by an intra-peritoneal injection of chlorhydrate (40 mg/100 g). The hair over the calvarium was shaved and cleaned with a depilator. A midline calvarial incision was made, and a 5-mm hole was drilled through the calvarial bone using a trephine burr. Extreme care was taken to avoid damaging the dura mater. The rats (2 × 12) with calvarial defects were randomly allocated to 4 groups (3 rats/group) according to scaffold type. Rats with critical-sized (5 mm) calvarial defects were implanted with either collagen scaffolds, collagen/RSV scaffolds, hASCs-cultured collagen scaffolds, or hASCs-cultured collagen/RSV scaffolds in the defect site. The wounds were sutured after implantation with nylon 3-0 sutures. All rats survived and had no wound infections throughout the experiment. The rats were sacrificed at 3 days (N = 3), 1 (N = 3), and 2 (N = 3) weeks after surgery. Calvarial specimens were harvested and then evaluated radiographically and histologically.

2.6 | Histological analysis

2.6.1 | Scanning electron microscopy (SEM)

The samples of biocomposites were fixed with 3.5% glutaraldehyde and washed in 0.33 M sucrose buffer at 4°C. After soaking in 1% osmium tetroxide, the samples were washed in 0.33 M sucrose buffer, followed by distilled water, and were then dehydrated in an ethanol/isoamylacetate gradient at 4°C. After reaching the drying critical point, the samples were attached to aluminium stubs and sputter coated with gold prior to examination with the HITACHI S-3000N

scanning electron microscope with an acceleration voltage at 10.0 kV.

2.6.2 | Immunohistochemistry

After fixing with 4% paraformaldehyde, the samples were sliced by cryosection. Each section (20 μ M) was treated with 0.2% Triton X-100 for 15 minutes, washed thrice with phosphate-buffered saline (PBS), blocked with 10% normal goat serum, and incubated with a primary antibody for 2 hours at room temperature. The primary antibodies used were Oct-4 (1:1000 dilution, polyclonal rabbit; ABGENT, San Diego, CA), Nestin (monoclonal mouse), Involucrin (polyclonal rabbit), and Osteocalcin (polyclonal goat) diluted to a ratio of 1:500 (Santa Cruz Biotechnology, CA). After washing thrice with PBS, the sections were incubated for 1 hour at room temperature with secondary antibody fluorescein isothiocyanate (FITC)-conjugated anti-rabbit, anti-mouse, or anti-goat, depending on the primary antibody (1:1000 dilution; ANASPEC, Fremont, CA). For visualisation of the nucleus, sections were incubated for 15 minutes with a 1:5000 dilution of Hoescht 33342 in PBS (Invitrogen, Thermo Fisher Scientific, Massachusetts). Fluorescent images were obtained with an epifluorescent microscope equipped with a SPOT-RT digital camera (Diagnostic Instruments, Detroit, MI).

2.6.3 | Flow cytometry

hASCs were added PBS for 5-minute shaking after they were collected from membranes by 0.25% trypsin-EDTA and FBS. hASCs were fixed with alcohol acetic acid solution (95% alcohol + 5% acetic acid) for 5 minutes. Then, hASCs were rinsed with PBS and punched with 0.05% NP-40 (diluted with PBS) for 10 minutes. After being rinsed with PBS, hASCs were blocked with 2% FBS for 10 minutes. After that, hASCs were added the primary antibody (except negative control) and kept in the fridge (40°C) overnight. The primary antibodies used in the experiment are Oct-4 and Osteocalcin. Then, the hASCs were rinsed with PBS and added the fluorescence antibody for 2 hours. The fluorescence antibodies that were used in this experiment are anti-rabbit-FITC and anti-goat-Rhodamine. After being rinsed with PBS, hASCs were fixed with 1% paraformaldehyde and analysed by flow cytometry machine (BD FACSCalibur, BD Biosciences, New Jersey).

2.6.4 | Alizarin red staining

The cultivation liquid was first removed and the sample was washed with PBS. Next, the sample was fixed for 30 minutes with 4% paraformaldehyde and washed again with PBS. The sample was stained with Alizarin red S solution until it turned reddish orange between 30 seconds and 5 minutes. Deionised water was then used to wash it several times to remove the staining liquid, and the sample was placed under microscope for observation.

2.6.5 | von Kossa staining

The cultivation liquid was removed and the sample was washed once with PBS. Afterwards, the sample was fixed for 30 minutes with 4% paraformaldehyde and washed again with PBS. Sections were incubated with 1% silver nitrate solution in a clear glass coplin jar and placed under ultraviolet light for 20 minutes (or in front of a 60-100 W light bulb for 1 hour or longer). The sections were then rinsed several times with distilled water, and non-reacted silver was removed with 5% sodium thiosulphate for 5 minutes. Finally, deionised water was used to wash it several times to remove the staining liquid, and the samples were placed under microscope for observation.

2.6.6 | Masson's trichrome staining

The paraffin-embedded blocks were cut into 5- μ m-thick sections and stained using a Masson's trichrome stain kit (Sigma Aldrich, Laborchemikalien GmbH, Hanover, Germany) according to the manufacturer's instructions (collagenous materials stained blue, whereas nuclei, fibres, erythrocytes, and elastins were stained red/pink).

2.6.7 | In vivo micro-computed tomography (μ CT)

At 3 months post-implantation, calvarial specimens were harvested and radiographically imaged using in vivo μ CT (SkyScan 1172; Bruker Micro-CT, Kontich, Belgium) and scanned at 65 kV/385 mA source voltage/current, with a 1-mm aluminium filter. The pixel size (resolution), rotation step, and exposure time were 35 μ m, 0.6° over 360°, and 400 ms, respectively. The μ CT analysis was performed with a software programme (CTAN, SkyScan; Bruker Micro-CT). Appropriate magnification was used throughout the observation, and the micrograph results were compared among groups; 3D images of the defect area were constructed using a CTVol Software Version 2.6, allowing for imaging rendering and visualisation.

2.7 | Ethical consideration

Rats were purchased from the Animal Laboratory Center for National Defense Medical Center, Taipei, Taiwan, and the in vivo experiments were performed with the approval of the National Defense Medical Center of Animal Care and Use Committee.

3 | RESULTS

3.1 | Stem cell morphology and distribution in scaffolds

Figure 1 displays SEM images of collagen scaffolds and collagen/RSV scaffolds. Upon isolation and purification of the hASCs, the stem cells were seeded on both scaffolds. After a 14-day incubation period, SEM analysis revealed

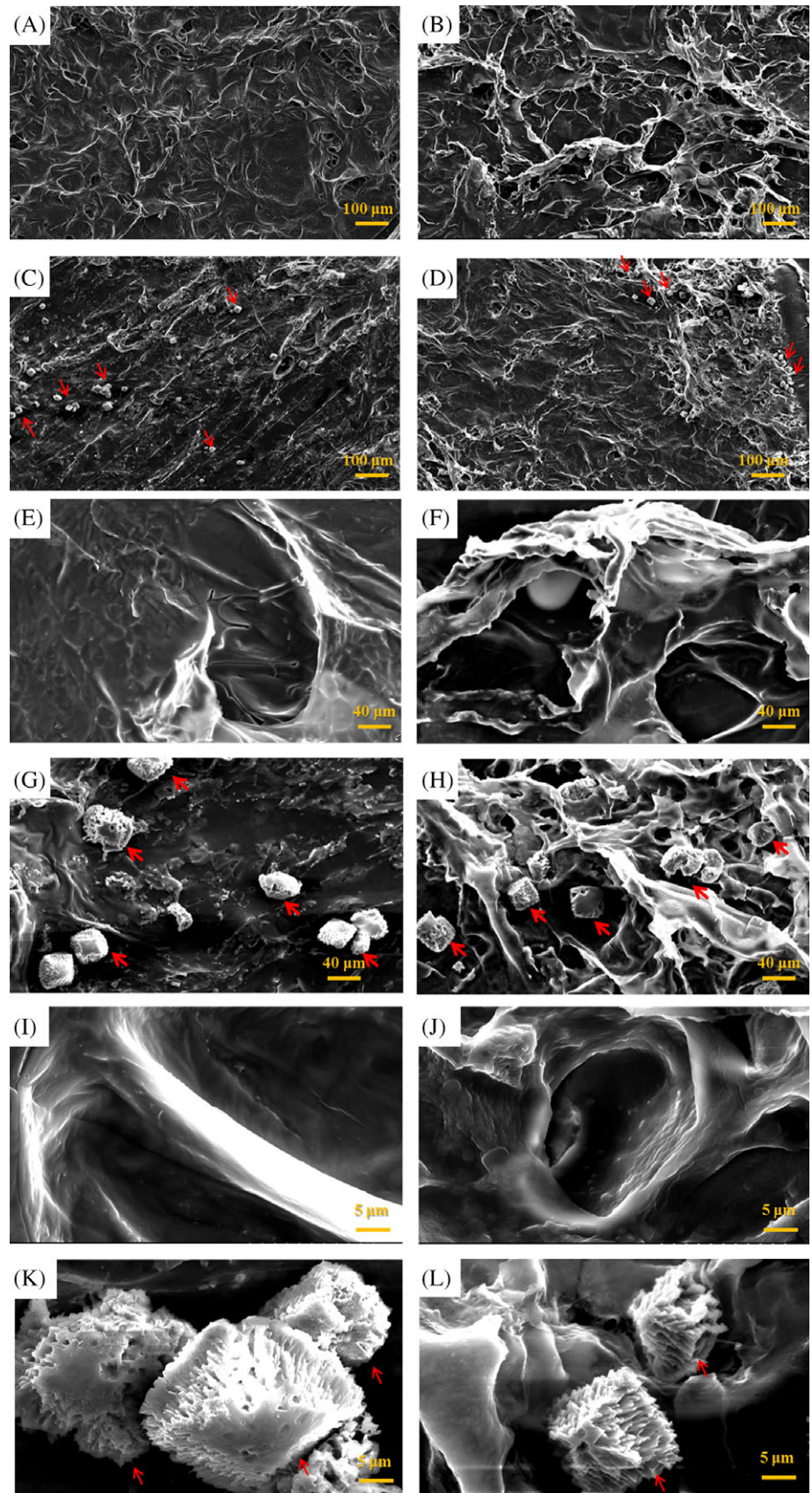


FIGURE 1 Scanning electron micrographs of a collagen scaffold (A, E, I), human adipose stem cells (hASCs) seeded on a collagen scaffolds (C, G, K), a collagen/RSV scaffolds (B, F, J), and hASCs seeded on a collagen/RSV scaffolds (D, H, L). Red arrows indicate cells. The surface of the collagen/RSV scaffolds is rougher and more creased than that of the collagen scaffolds. Both scaffolds exhibit excellent cell compatibility. Scale bar = 100 μm (A–D); 20 μm (E–H); 5 μm (I–L)

that the seeded cells grew on and adhered well to the scaffolds, covering their pores. This result implies that both scaffolds are biocompatible for ex vivo stem cell attachment. By comparing the SEM images of a collagen

scaffold (Figure 1A,E,I), hASCs on a collagen scaffold (Figure 1C,G,K), a collagen/RSV scaffold (Figure 1B,F,J), and hASCs on a collagen/RSV scaffold (Figure 1D,H,L), we observed that the surface of the collagen/RSV scaffold

is rougher and more creased than that of the collagen scaffold. Both scaffolds exhibit high compatibility with hASCs.

3.2 | RSV release test

Collagen scaffolds containing RSV were prepared and subjected to controlled release analysis using a collagen scaffold as the control. The scaffolds were immersed in a 50-mL solution of artificial saliva for 150 minutes and sampled at 30-minute intervals. The RSV concentration in the samples was measured by spectrophotometry at 350 nm using a calibration curve. Figure 2 shows that the collagen/RSV scaffold released over twice as much RSV as the blank collagen scaffold did.

3.3 | Cell phenotype assessment

Immunocytochemical staining revealed the expression of Oct-4, Nestin, CK-14, and Osteocalcin. For nucleus visualisation, sections were incubated with Hoescht 33342 in phosphate-buffered saline. Fourteen days after differentiation, some cells exhibited epithelial cell and osteocyte morphological characteristics. Immunostains of hASCs cultured on collagen/RSV scaffolds exhibited a greater degree of cell differentiation than on collagen scaffolds in both media. Immunocytochemical staining showed that these cells expressed the epithelial marker CK-14 (Figure 3E,F) and the bone formation marker Osteocalcin (Figure 3G,H). We also observed retention of the stem cell markers Oct-4 (Figure 3A,B) and Nestin (Figure 3C,D) after biocomposite formation.

3.4 | Flow cytometry analysis

hASCs grown in collagen scaffold (Figure 4A,C) and collagen scaffold/RSV (Figure 4E,G) with stem cell medium culture and immunofluorescent staining with Osteocalcin. The dot plots on hASCs for the double staining of Oct-4 and Osteocalcin. The fluorescence intensity of each FITC-labelled Oct-4 is non-represented on the X-axis, and the percentages represent the bone differentiation of hASCs in each scaffolds (Figure 4B,D,F,H).

3.5 | Osteogenic differentiation

We carried out a histological analysis using Alizarin red and von Kossa staining to visualise the mineralisation of hASC osteogenic differentiation in the collagen scaffolds and collagen/RSV scaffolds. When cultured in osteogenic-inducing medium, calcium deposits were found on both collagen scaffolds and collagen/RSV scaffolds, as shown in Figure 5A,B. The results showed statistical significance at $P < .001$ for comparison of collagen scaffolds and collagen/RSV scaffolds vs 24-well plates.

3.6 | Healing of oral mucosal lesions

After confirmation of induction, we applied the collagen scaffolds and collagen/RSV scaffolds in a rat model of tongue defects. Figure 6A-C depicts the steps for epithelium flap removal. We observed and recorded wound healing daily. For both the collagen scaffold (Figure 6D-F) and collagen/RSV scaffold (Figure 6G-I) graft, an epithelium-like layer covered the wound. After 14 days, the wound became smooth and almost completely healed.

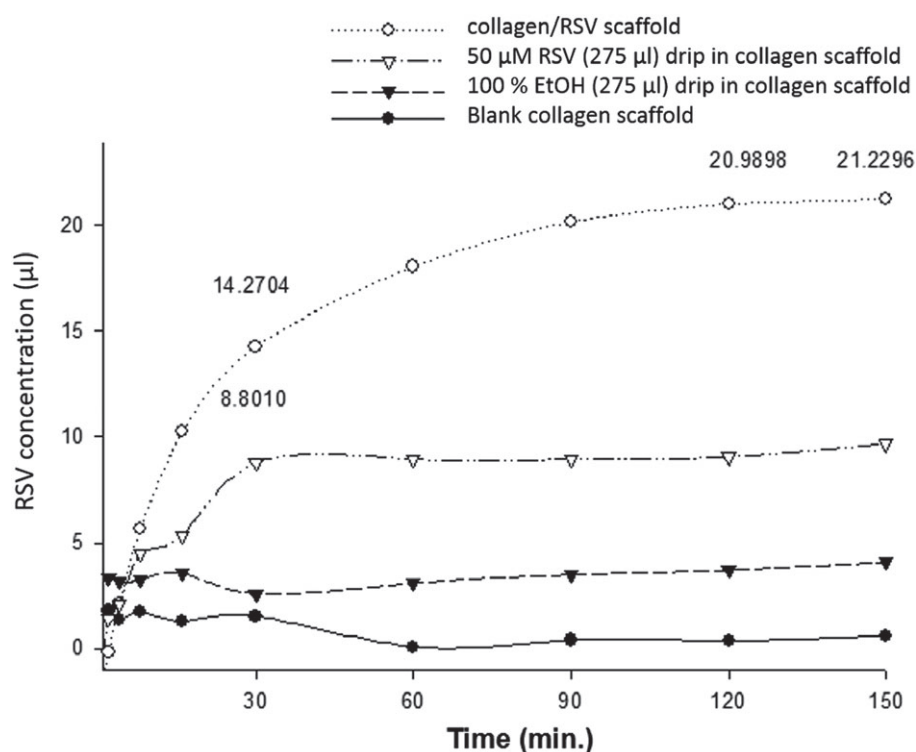


FIGURE 2 Controlled release analysis results for RSV from collagen scaffolds in artificial tissue fluid as artificial saliva. The RSV-containing collagen scaffolds released over twice as much RSV as did the RSV drip in the collagen scaffolds after 60 minutes. (Sample number: 3 wells; number of analysed images: 5)

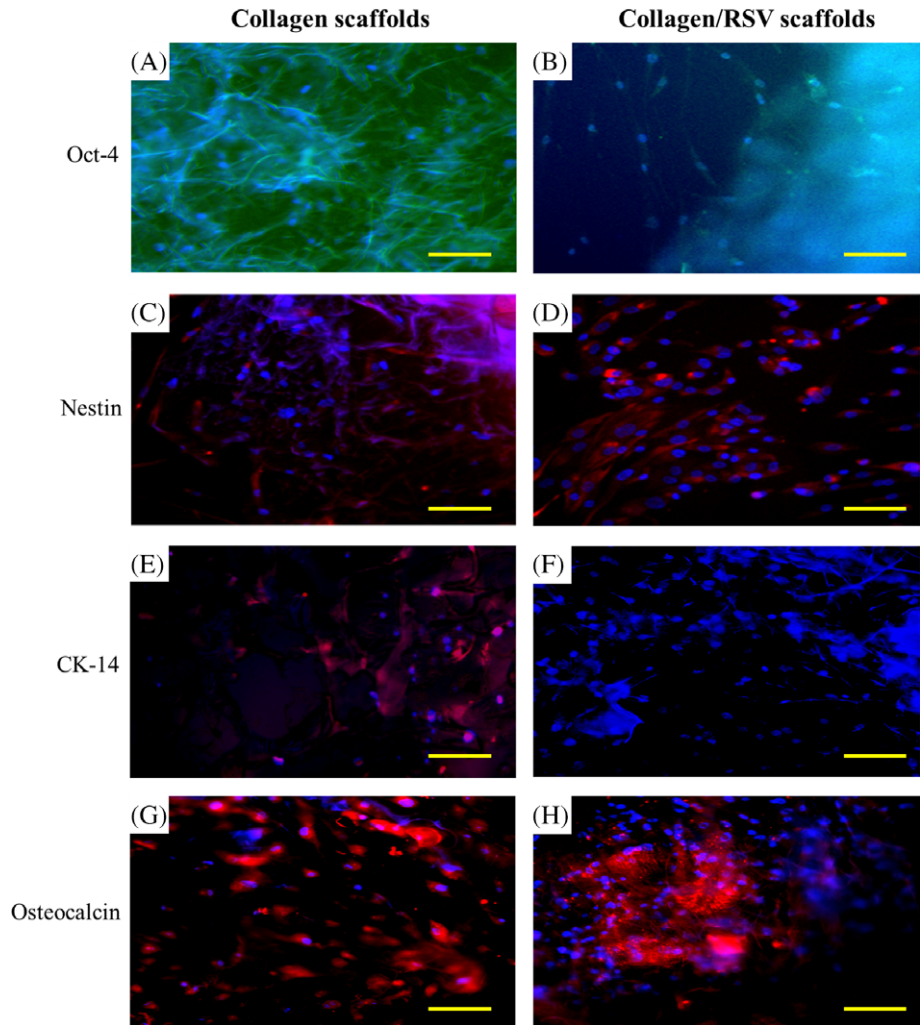


FIGURE 3 Representative scanning electron microscopy micrographs of (A) collagen scaffold + hASCs and (B) collagen/RSV + hASCs. Differentiation potential of hASCs via scaffold induced for 14 days. All blue depicts cell nuclei stain (Hoechst 33342); green and red depicts expression of lineage specific marker. (C, D) Neurogenesis (Nestin), (E, F) epithelial differentiation (Involucrin), (G, H) chondrogenesis (SOX9), (I, J) osteogenesis (Osteocalcin). Red arrow indicated hASCs existent)

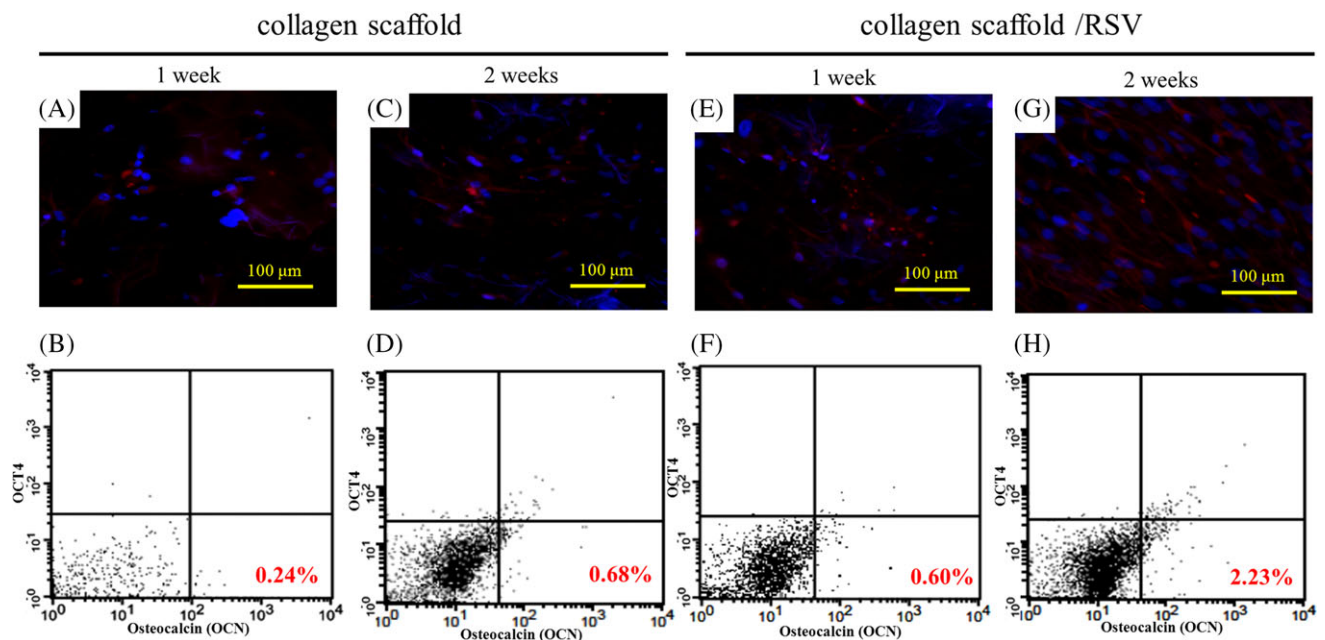


FIGURE 4 The osteogenic characteristics of hASCs grown in collagen scaffold and collagen/RSV for 1 and 2 weeks. (A, C, E, G) Immunofluorescent staining of Osteocalcin was visualised with the HiLyte Fluor 594-labelled secondary antibody, which is shown in red. Nuclei that were counterstained with Hoechst 33 342 are shown in blue. (B, D, F, H) The flow cytometric analysis of embryonic stem cell-associated protein expression and osteigenesis marker. Representative dot plots for the double staining of Oct-4 and Osteocalcin. The fluorescence intensity of each FITC-labelled Oct-4 is not represented on the X-axis; the percentages represent the bone differentiation of hASCs in each scaffolds

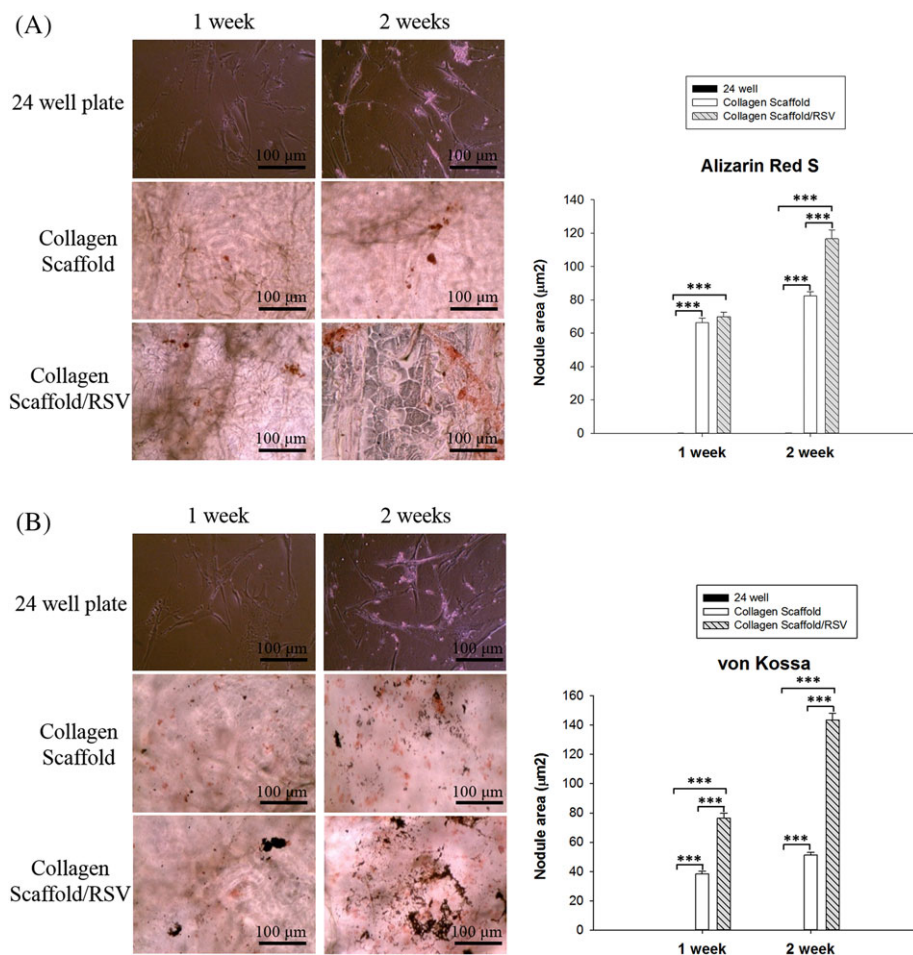


FIGURE 5 Mineralisation evaluation of hASCs grown in collagen scaffold and collagen scaffold/RSV for 1 and 2 weeks. Measurement of nodule area (μm^2) represents mineralization deposition in each scaffold. (A) Calcium deposition of hASCs cultured in each scaffold in Alizarin red staining. (B) Phosphate deposition with von Kossa staining

In the histological analysis of tongue defect healing, we observed wound healing by Masson's trichrome staining and compared the immunofluorescence staining 14 days after surgery. Figure 7A-C displays the lesion control group, as well as the collagen scaffolds and collagen/RSV scaffolds.

The red arrows in Figure 7 pinpoint the lesion site. The collagen deposit is clearly visible in the collagen and collagen/RSV scaffold groups. For the collagen/RSV group, the wound displays reepithelialisation and multi-layers denser than those seen in the other 2 groups. Immunofluorescence

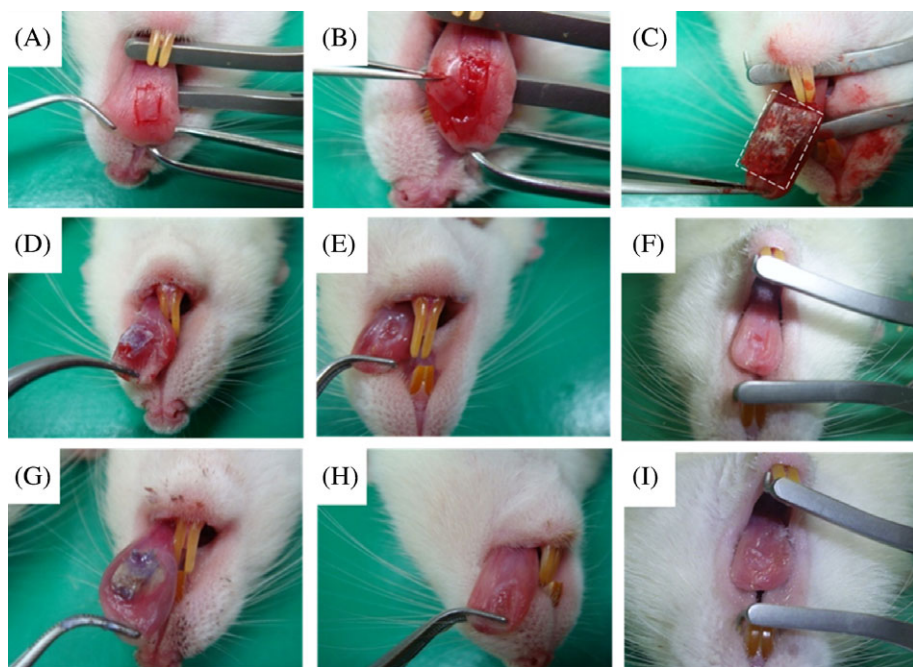


FIGURE 6 Tongue mucosal wound healing. The debridement procedure of collagen scaffold and collagen/RSV scaffold covering the rat tongue (A-C). Both the collagen scaffold (D-F) and collagen/RSV scaffold (G-I) showed good coverage of the underside of the tongue defect (D, G) 3 days, (E, H) 7 days, (F, I) 14 days after surgery. (Sample number: 5 of each group)

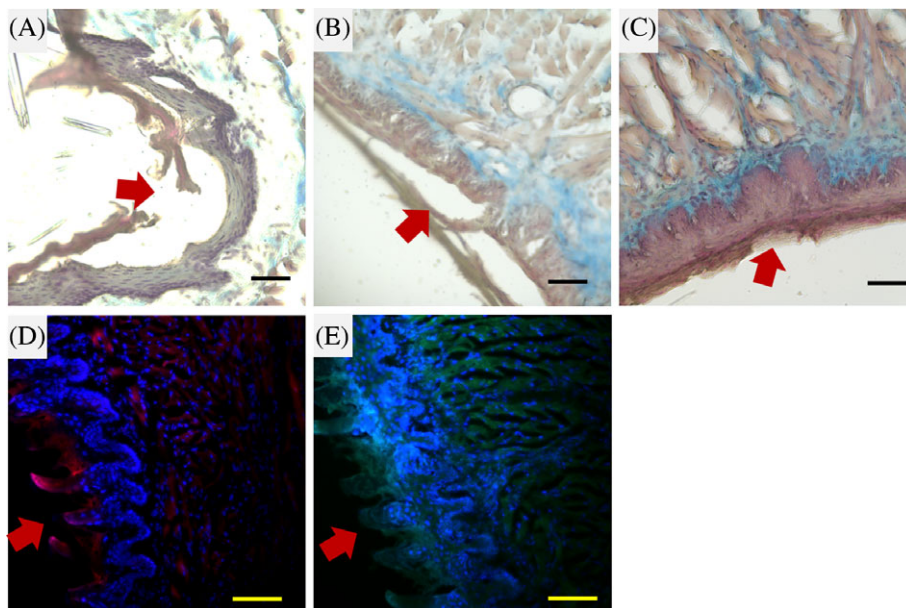


FIGURE 7 Histological observation of a tongue defect in a rat model. Wound edges with Masson's trichrome stain for the lesion control group (A), collagen scaffold covered group (B), and collagen/RSV scaffold covered group (C) 14 days after surgery. Immunohistochemical stains of CK-14 (D) and Involucrin (E) at the wound edge of the collagen/RSV scaffold covered group 14 days after surgery. Red arrows indicate the defect margins. Scale bar = 50 μm (A–C) and 100 μm (D, E)

staining confirmed the presence of both keratinocyte markers CK-14 (Figure 7D) and Involucrin (Figure 7E) that were expressed on the regrowth area of the defect margins.

3.7 | Reconstruction of rat calvarial defects

Sprague-Dawley rats that had undergone calvarial defect surgery were sacrificed at 3 months and were evaluated radiographically. Calvarial defects in the rat models reveal that osteoinduced hASCs on collagen/RSV scaffolds provide the most effective means of regenerating bone. The μCT images show bone regeneration after 3 months for hASCs and osteoinduced hASCs on collagen and collagen/RSV scaffolds. One group was used to compare collagen and collagen/RSV scaffolds. For the other groups, the left hole without a scaffold was used as a control. The rendered and visualised μCT images indicate that the collagen/RSV scaffold is more effective at bone regeneration than that of the collagen scaffold (Figure 8A). Further comparison of the results showed improved bone mineralisation in the case of the seeded stem cells (Figure 8B,C) and osteoinduced stem cells (Figure 8D) on the collagen/RSV scaffold. Among the 3 cases (Figure 8B–D), the hASCs on a collagen/RSV scaffold displayed the best results (Figure 8C). Furthermore, it is also noted that the collagen scaffold case showed more bone fill than that of the empty site, which indicated its comparatively better performance over the non-treatment case.

4 | DISCUSSION

RSV stimulates osteoblastogenesis and inhibits osteoclast activation *in vitro*. A previous work²⁵ reported that RSV stimulates mRNA expression of Osteocalcin and Osteopontin in immortalised osteoblast-like hMSC-TERT cells in a

dose-dependent manner. Mizutani et al²⁶ demonstrated that RSV enhances the proliferation and differentiation of mouse osteoblastic MC3T3 cells. We prepared a novel bio-composite that combines RSV and collagen by using a freeze-dry protocol for the first time. The results in our *in vitro* study demonstrate that the collagen/RSV scaffold is an effective biomaterial for oral and cranial tissue reconstruction. Both collagen and collagen/RSV scaffolds showed high compatibility with hASCs, but the latter scaffold was twice as effective as the former in releasing RSV. Figure 1 shows that hASCs strongly adhered to and proliferated on both scaffolds. Furthermore, there was increased cell adhesion, as well as restricted cell growth and spread, on the scaffold surfaces used for tissue engineering. This result suggests that the collagen/RSV scaffold is more effective at wound healing than the collagen scaffold because it is biocompatible and releases a higher concentration of RSV, which, in turn, aids in wound contraction and closure.

Immunohistochemical analysis showed greater cell differentiation on collagen/RSV scaffolds than on collagen scaffolds under both stem cell- and osteogenesis-inducing media. The increased cell differentiation on collagen/RSV scaffolds may be attributed to the higher concentration of released RSV compared with that on collagen scaffolds in the same period, which promote the osteogenesis of hASCs. Both scaffolds displayed positive expression of calcium deposits, implying that the hASCs cultured on both scaffolds had differentiated in the osteogenesis-inducing medium (Figure 5A). Hence, both scaffolds could potentially be used in the treatment of critical bone defects. However, as the immunohistochemical analysis showed greater cell differentiation on collagen/RSV scaffolds than on collagen scaffolds, the collagen/RSV scaffold is probably more effective for this purpose. Notably, hASCs were seeded in stem cell medium only for 1 week, and they were 0.24%

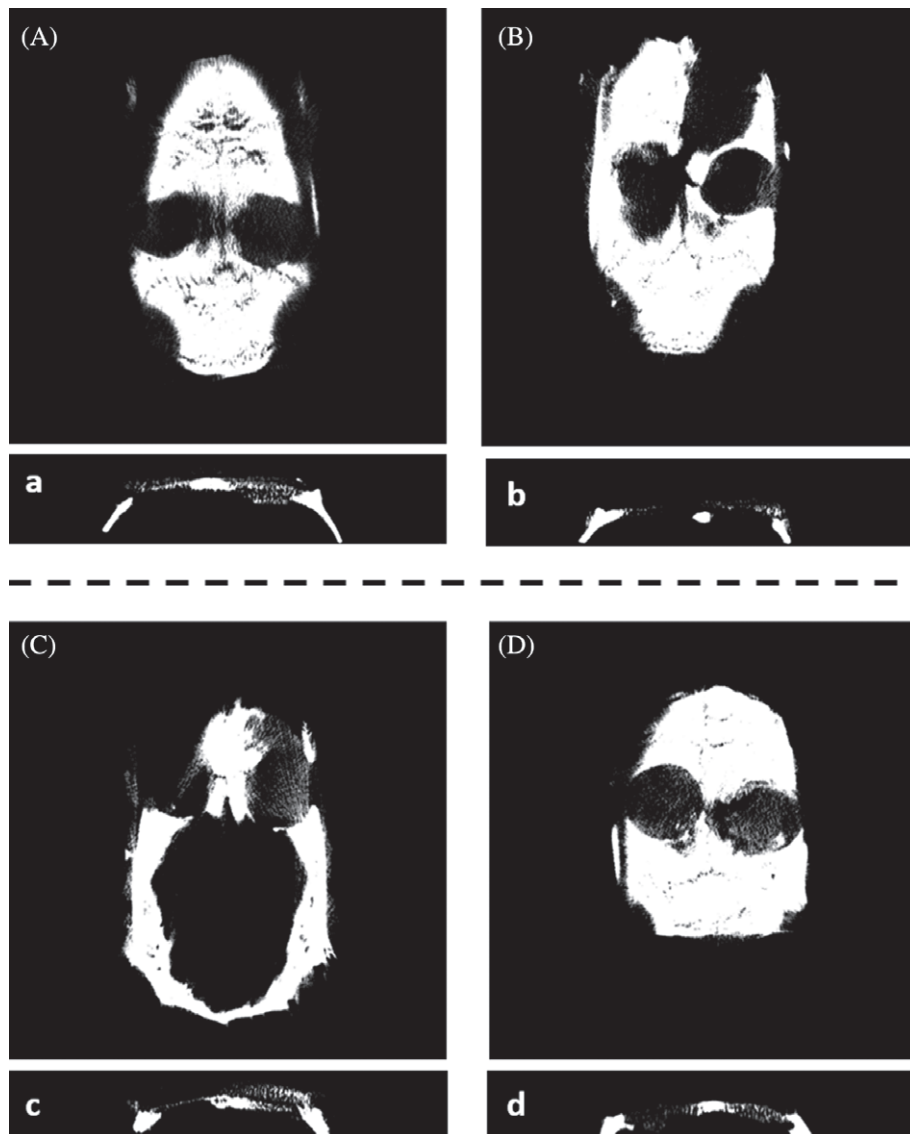


FIGURE 8 In vivo μ CT images of a rat model for calvarial defects scanned at 3 months: defects treated with (A) a collagen scaffold (left) and a collagen/RSV scaffold (right). (B) An empty defect (left) and hASCs on a collagen scaffold (right); (C) an empty defect (left) and an hASCs on a collagen/RSV scaffold (right); and (D) empty defect (left) and osteoinduced hASCs on a collagen scaffold (right)

positive with Osteocalcin marker on collagen scaffolds and 0.60% on collagen/RSV scaffold because RSV supported osteogenic differentiation of hASCs (Figure 4). There are a few hASCs that demonstrated the presence of Oct-4 marker when they were seeded on collagen scaffolds and collagen/RSV scaffold under stem cell medium culture. However, the percentage of hASCs displayed positively with Osteocalcin on collagen scaffolds and collagen/RSV scaffold increased from 0.24% to 0.68% and from 0.60% to 2.23% under the stem cell medium culture, respectively. Thus, the collagen/RSV scaffold enables a more effective application of RSV-based treatments because it allows the 2-fold release of RSV, which amplifies osteogenesis, even though both scaffolds display good biocompatibility with hASCs and promote osteogenesis.

In vivo experiments on oral mucosal lesion demonstrated that the collagen/RSV scaffold is more effective in wound closure and contraction than the collagen scaffold (Figures 6 and 7). We chose a 14-day experiment to compare the histology using Masson's trichrome staining

(a method for visualising collagen and proteoglycans), which we confirmed by in vivo immunofluorescence. Collagen deposits were abundant in the collagen and collagen/RSV scaffold groups. The wound that had been treated using the collagen/RSV scaffold exhibited denser, epithelialisation and multi-layers compared with those of the other 2 groups. Immunofluorescence images confirm the expression of keratinocyte markers, Involucrin, and CK-14 on the regrowth area of the defect margins in the collagen/RSV group.

The μ CT images show regenerating bone in defects covered with hASCs on a collagen/RSV scaffolds that are more visible than that in defects covered with hASCs on collagen scaffolds (Figure 8). This supports our previous finding that the collagen/RSV scaffold is more effective at regenerating bone than the collagen scaffolds. We therefore conclude that the collagen/RSV scaffold seeded with osteogenically differentiated hASCs would be more effective in the treatment because hASCs induce osteoblasts before implantation. This effect, with the aid of RSV, would

result in a higher percentage of osteogenesis. RSV reduces levels of pro-inflammatory cytokines, thus inhibiting PAP and P2-receptor signalling through MAPK, cJun, and JNK. It promotes an anti-inflammatory response^{27,30} by inhibiting PG synthesis through the inhibitory effect of cyclooxygenase-1 with RSV.³¹ We thus believe that collagen/RSV scaffolds facilitate epithelium repair, while RSV inhibits proliferation and increases differentiation of osteoblasts from stem cells. Therefore, the strong anti-inflammatory effects of RSV offer a potential treatment for craniofacial degenerative diseases.

5 | CONCLUSIONS

Using collagen/RSV biocomposite scaffolds in stem cell differentiation, we demonstrate for the first time that RSV is highly biocompatible and yields high differentiation rates of stem cells and osteogenesis in epithelium-inducing media in vitro. hASCs cultured in vitro on the collagen/RSV scaffold exhibited calcium deposits, which is further evidence of RSV's ability to promote osteogenesis. The in vivo results also indicate the high biocompatibility of collagen/RSV scaffolds and their great effectiveness in promoting epidermal wound healing. In addition, RSV-induced osteogenesis of hASCs and osteoinduced hASCs seeded on the collagen scaffolds led to near-complete bone regeneration and coverage of calvarial defects. Results of this experiment therefore suggest that RSV-containing collagen biomaterials are more effective than collagen scaffolds at enhancing the epithelial and osteogenic differentiation of hASCs. This study developed a feasible procedure for future clinical applications using collagen/RSV scaffolds for tissue engineering for craniofacial defect reconstruction.

ACKNOWLEDGEMENTS

This research was supported by Defense Technology Cooperative Research: 105-2623-E-016-004-D; Ministry National Defense-Medical Affairs Bureau: MAB-105-041; Tri-Service General Hospital ROC program: TSGH-C97-109, TSGH-C99-129, TSGH-C103-037, TSGH-C104-098, TSGH-C106-074. We wish to acknowledge the help given by Dr Chuan-Chung Chuang, DDS, in providing the adipose tissue of samples from dental surgery in a clinical setting.

ORCID

Shu-Jen Chang  <http://orcid.org/0000-0001-6203-057X>

REFERENCES

- Iida T, Takami Y, Yamaguchi R, Shimazaki S, Harii K. Development of a tissue-engineered human oral mucosa equivalent based on an acellular allogeneic dermal matrix: a preliminary report of clinical application to burn wounds. *Scand J Plast Reconstr Surg Hand Surg*. 2005;39:138-146.
- D'Aquino R, De Rosa A, Lanza V, et al. Human mandible bone defect repair by the grafting of dental pulp/stem progenitor cells and collagen sponge biocomplexes. *Eur Cell Mater*. 2009;18:75-83.
- Laurell L, Gottlow J, Zybutz M, Persson R. Treatment of intrabony defects by different surgical procedures. A literature review. *J Periodontol*. 1998;69:303-313.
- Phillips JH, Forrest CR, Gruss JS. Current concepts in the use of bone grafts in facial fractures. Basic science considerations. *Clin Plast Surg*. 1992;19:41-58.
- Huang YC, Kaigler D, Rice KG, Krebsbach PH, Mooney DJ. Combined angiogenic and osteogenic factor delivery enhances bone marrow stromal cell-driven bone regeneration. *J Bone Miner Res*. 2005;20:848-857.
- Krebsbach PH, Kuznetsov SA, Satomura K, Emmons RV, Rowe DW, Robey PG. Bone formation in vivo: comparison of osteogenesis by transplanted mouse and human marrow stromal fibroblasts. *Transplantation*. 1997;63:1059-1069.
- Hong L, Mao JJ. Tissue-engineered rabbit cranial suture from autologous fibroblasts and BMP2. *J Dent Res*. 2004;83:751-756.
- Jin Q, Anusaksathien O, Webb SA, Printz MA, Giannobile WV. Engineering of tooth-supporting structures by delivery of PDGF gene therapy vectors. *Mol Ther*. 2004;9:519-526.
- Kuo TF, Huang AT, Chang HH, Lin FH, Chen ST, Chen RS. Regeneration of dentin-pulp complex with cementum and periodontal ligament formation using dental bud cells in gelatin-chondroitin-hyaluronan tri-copolymer scaffold in swine. *J Biomed Mater Res*. 2008;86:1062-1068.
- Schek RM, Taboas JM, Hollister SJ, Krebsbach PH. Tissue engineering osteochondral implants for temporomandibular joint repair. *Orthod Craniofac Res*. 2005;8:313-319.
- Tremp M, Eberli D, Gobet R, Salemi S, Sulser T. Adipose-derived stem cells (ASCs) for tissue engineering. In Eberli D, ed. *Regenerative Medicine and Tissue Engineering—Cells and Biomaterials*. Vol 7. London, UK: InTech; 2011:179-194.
- Itoi Y, Takatori M, Hyakusoku H, Mizuno H. Comparison of readily available scaffolds for adipose tissue engineering using adipose-derived stem cells. *J Plast Reconstr Aesthet Surg*. 2010;63(5):858-864.
- Yamada Y, Boo JS, Ozawa R, et al. Bone regeneration following injection of mesenchymal stem cells and fibrin glue with a biodegradable scaffold. *J Craniomaxillofac Surg*. 2003;31(1):27-33.
- Langer R, Vacanti JP. Tissue engineering. *Science*. 1993;260(5110):920-926.
- Altman AM, Yan Y, Matthias N, et al. Human adipose-derived stem cells seeded on a silk fibroin-chitosan scaffold enhance wound repair in a murine soft tissue injury model. *Stem Cells*. 2009;27(1):250-258.
- Stefan L, Andreas J, Petros C, et al. Autologous stem cells (adipose) and fibrin glue used to treat widespread traumatic calvarial defects: case report. *J Craniomaxillofac Surg*. 2004;32(6):370-373.
- Lucas C, Criens-Poublon LJ, Cockrell CT, Haan RJ. Wound healing in cell studies and animal model experiments by low level laser therapy; were clinical studies justified? A systematic review. *Lasers Med Sci*. 2002;17:110-134.
- Babior BM. Phagocytes and oxidative stress. *Am J Med*. 2000;109:33-44.
- Babior BM, Lambeth JD, Nauseef W. The neutrophil NADPH oxidase. *Arch Biochem Biophys*. 2002;397:342-344.
- Klyubin IV, Kirpichnikova KM, Gamaley IA. Hydrogen peroxide-induced chemotaxis of mouse peritoneal neutrophils. *Eur J Cell Biol*. 1996;70:347-351.
- de la Lastra CA, Villegas I. Resveratrol as an antioxidant and pro-oxidant agent: mechanisms and clinical implications. *Biochem Soc Trans*. 2007;35:1156-1160.
- Losa GA. Resveratrol modulates apoptosis and oxidation in human blood mononuclear cells. *Eur J Clin Invest*. 2003;33:818-823.
- Bäckesjö CM, Li Y, Lindgren U, Haldosén LA. Activation of Sirt1 Decreases Adipocyte Formation during Osteoblast Differentiation of Mesenchymal Stem Cells. *Cells Tissues Organs*. 2009;189:93-97.
- Tseng PC, Hou SM, Chen RJ, et al. Resveratrol promotes osteogenesis of human mesenchymal stem cells by upregulating RUNX2 gene expression via the SIRT1/FOXO3A axis. *J Bone Miner Res*. 2011;26(10):2552-2563.
- Boissy P, Andersen TL, Abdallah BM, Kassem M, Plesner T, Delaisse JM. Resveratrol inhibits myeloma cell growth, prevents osteoclast

- formation, and promotes osteoblast differentiation. *Cancer Res.* 2005;65:9943-9952.
26. Mizutani K, Ikeda K, Kawai Y, Yamori Y. Resveratrol stimulates the proliferation and differentiation of osteoblastic MC3T3-E1 cells. *Biochem Biophys Res Commun.* 1998;253:859-863.
 27. Cherng JH, Chang SJ, Yeh JZ, et al. Development of fabrication technique in nano-scale resveratrol by collagen. *Int J Nanotechnol.* 2013;10:984-995.
 28. Cherng JH, Chang SJ, Fang TJ, et al. Surgical-derived oral adipose tissue provides early stage adult stem cell. *J Dental Sci.* 2014;9(1):10-15.
 29. Cherng JH, Chang SC, Chen SG, et al. The effect of hyperbaric oxygen and air on cartilage tissue engineering. *Ann Plast Surg.* 2012;69(6):650-655.
 30. Ornstrup MJ, Harsløf T, Sørensen L, Stenkjær L, Langdahl BL, Pedersen SB. Resveratrol increases osteoblast differentiation in vitro independently of inflammation. *Calcif Tissue Int.* 2016;99(2):155-163.
 31. Das S, Das DK. Anti-inflammatory responses of resveratrol. *Inflamm Allergy Drug Targets.* 2016;6(3):168-173.

How to cite this article: Wang C-C, Wang C-H, Chen H-C, et al. Combination of resveratrol-containing collagen with adipose stem cells for craniofacial tissue-engineering applications. *Int Wound J.* 2018;15:660–672. <https://doi.org/10.1111/iwj.12910>